J Neurophysiol 91: 274–285, 2004.
First published September 24, 2003; 10.1152/jn.00763.2003.

Telencephalic Input to the Pretectum of Pigeons: An Electrophysiological and Pharmacological Inactivation Study

Nathan A. Crowder,[2] Clayton T. Dickson,[1,2] and Douglas R.W. Wylie[1,2]
[1]*Department of Psychology and* [2]*Centre for Neuroscience, University of Alberta, Edmonton, Alberta T6G 2E9, Canada*

Submitted 6 August 2003; accepted in final form 20 September 2003

Crowder, Nathan A., Clayton T. Dickson, and Douglas R.W. Wylie. Telencephalic input to the pretectum of pigeons: an electrophysiological and pharmacological inactivation study. *J Neurophysiol* 91: 274–285, 2004. First published September 24, 2003; 10.1152/jn.00763.2003. The pretectal nucleus lentiformis mesencephali (LM) and the nucleus of the basal optic root (nBOR) of the avian accessory optic system (AOS) are retinal-recipient visual nuclei involved in the analysis of optic flow that results from self-motion, and in the generation of the optokinetic response. Neurons in these nuclei show direction selectivity in response to large-field motion and are tuned in the spatiotemporal domain. In addition to retinal afferentation, both the nBOR and LM receive afferents from the Wulst, which is thought to be the avian homolog of the primary visual cortex. We examined the effects of Wulst electrical stimulation on the activity of LM neurons and recorded the directional and spatiotemporal tuning of LM neurons in pigeons before, during, and after the Wulst was temporarily inactivated by lidocaine injection. In response to Wulst electrical stimulation, LM neurons showed either short-latency excitation followed by longer-latency inhibition (W+ cells), or only a longer-latency inhibition (W− cells). The average response latencies for W+ and W− cells were 13.5 and 28.3 ms, respectively. The effects of Wulst stimulation did not correlate with either the directional or spatiotemporal tuning of the LM neurons. Injection of lidocaine into the nBOR reduced the longer-latency oscillations of W+ and W− cells. When the Wulst was temporarily inactivated by lidocaine neither the directional nor spatiotemporal response properties of LM neurons were affected. The possible functions of the projection from the Wulst to the LM are discussed.

INTRODUCTION

The pretectum and accessory optic system (AOS) are involved in the generation of the optokinetic response (OKR) and the processing of optic flow that results from self-motion (Gibson 1954; Grasse and Cynader 1990; Simpson 1984; Simpson et al. 1988). The OKR facilitates retinal image stabilization, which is important for optimal visual acuity (Carpenter 1977; Westheimer and McKee 1973) and velocity discrimination (Nakayama 1981).

The AOS and pretectum are highly conserved in vertebrates. The medial and lateral terminal nuclei (MTN, LTN) of the mammalian AOS are homologous to the avian nucleus of the basal optic root (nBOR), and the pretectal nucleus of the optic tract (NOT) in mammals is homologous to the nucleus lentiformis mesencephali (LM) in birds (Fite 1985; McKenna and Wallman 1985a; Simpson 1984; Simpson et al. 1988; Weber 1985). AOS and pretectal neurons have large receptive fields in the contralateral visual field and exhibit direction selectivity to drifting large-field visual stimuli. Most neurons in the LM and NOT prefer temporal-to-nasal (T-N) motion (NOT: Collewijn 1975a,b; Distler and Hoffmann 1993; Hoffmann and Distler 1989; Hoffmann and Schoppmann 1975, 1981; Hoffmann et al. 1988; Ibbotson et al. 1994; Ilg and Hoffmann 1996; Mustari and Fuchs 1990; Volchan et al. 1989; Yakushin et al. 2000; LM: Fan et al. 1995; Fite et al. 1989; Katte and Hoffmann 1980; McKenna and Wallman 1985b; Winterson and Brauth 1985; Wylie and Crowder 2000; Wylie and Frost 1996). In mammals, AOS neurons prefer upward or downward motion (e.g., Grasse and Cynader 1982, 1984; Simpson et al. 1979; Soodak and Simpson 1988), whereas nBOR neurons prefer upward, downward, or nasal-to-temporal motion (Burns and Wallman 1981; Gioanni et al. 1984; Morgan and Frost 1981; Rosenberg and Ariel 1990; Wylie and Frost 1990). When drifting sine-wave gratings are used as visual stimuli, neurons in the pretectum and AOS exhibit tuning in the spatiotemporal domain, preferring either high spatial frequencies (SFs) and low temporal frequencies (TFs), or low SFs and high TFs. Because velocity = TF/SF, these 2 groups were referred to as "slow" and "fast" neurons, respectively (Crowder and Wylie 2001; Crowder et al. 2003; Ibbotson and Price 2001; Ibbotson et al. 1994; Wylie and Crowder 2000).

Both the AOS and pretectum receive massive retinal input (Mammals: Garey and Powell 1968; Giolli and Guthrie 1969; Hayhow et al. 1960; Scalia and Arango 1979; Birds: Fite et al. 1981; Gamlin and Cohen 1988a; Karten et al. 1977; Reiner et al. 1979). However, the AOS and pretectum also receive numerous extraretinal inputs that could influence the visual response properties of neurons within these nuclei. For example, there is a heavy reciprocal connection between the AOS and pretectum (Rats: Blanks et al. 1982; Terasawa et al. 1979; Rabbits: Giolli et al. 1984; Holstege and Collewijn 1982; Cats: Berson and Graybiel 1980; Itoh 1977; Weber and Harting 1980; Pigeons: Brecha et al. 1980; Clarke 1977; Gamlin and Cohen 1988b; Wylie et al. 1997). Furthermore, the AOS and pretectum receive input from the telencephalon, although this input is quite variable between species. In cats and monkeys, the cortical input to NOT is quite heavy (Hoffmann et al. 1991; Ilg and Hoffmann 1993; Mustari et al. 1994; Schoppmann 1981), but is absent in other frontal-eyed species such as the opossum (Pereira et al. 2000). Moreover, the NOT receives cortical input in rabbits (Hollander et al. 1979), guinea pigs (Lui et al. 1994), and rats (Shintani et al. 1999), but not in hamsters (Lent 1982) or tree shrews (Huerta et al. 1985). In pigeons, both the nBOR and LM receive afferents from the

Address for reprint requests and other correspondence: D. R. Wong-Wylie, Department of Psychology, University of Alberta, Edmonton, Alberta T6G 2E9, Canada (E-mail: dwylie@ualberta.ca).

The costs of publication of this article were defrayed in part by the payment of page charges. The article must therefore be hereby marked "*advertisement*" in accordance with 18 U.S.C. Section 1734 solely to indicate this fact.

Wulst (Miceli et al. 1979; Rio et al. 1983), which is thought to be the avian homolog of primary visual cortex (Karten and Shimizu 1989; Medina and Reiner 2000).

In the present study we used electrical stimulation and reversible pharmacological inactivation of the Wulst to ask the following questions about the LM. Is the Wulst projection to LM excitatory or inhibitory? Do both fast and slow LM cells receive input from the Wulst? Is the connection correlated with direction preference? Finally with the Wulst inactivation, we sought to determine whether the afferents from the Wulst contribute to the directional and spatiotemporal tuning of LM neurons.

METHODS

Surgery and extracellular recording

The methods used conformed to the guidelines established by the Canadian Council on Animal Care and were approved by the Biological Sciences Animal Welfare and Policy Committee at the University of Alberta. Details for anesthesia, extracellular recording, stimulus presentation, and data analysis were previously described by Wylie and Crowder (2000). Briefly, pigeons were anesthetized with a ketamine (65 mg/kg)–xylazine (8 mg/kg) mixture (intramuscularly), and supplemental doses were administered as necessary. Based on the pigeon stereotaxic atlas (Karten and Hodos 1967), sufficient bone and dura were removed to expose the brain and allow access to the LM, nBOR, and Wulst with vertical penetrations. Recordings were made with glass micropipettes filled with 2 M NaCl and Pontamine sky blue (tip diameters 4–5 microns). The extracellular signal was amplified, filtered, displayed on an oscilloscope, and fed to a window discriminator. TTL pulses representing single spikes were fed to a 1401*plus* [Cambridge Electronic Designs (CED)] and peristimulus time histograms (PSTHs) were constructed with *Spike2* software (CED).

Visual stimulus presentation

After neurons in the LM were isolated, the direction preference and the approximate locations of the receptive field boundaries and hot spot were qualitatively determined by moving a large (90° × 90°) handheld stimulus in various areas of the visual field. Directional and spatiotemporal tuning were determined quantitatively with sine-wave gratings that were generated by a VSG*Three* graphics computer (Cambridge Research Designs, Cambridge, UK), and back-projected onto a tangent screen that was located 50 cm from the bird (90° × 75°). Direction tuning was tested using gratings of an effective SF and TF at 22.5° increments. Direction preference was quantitatively assigned by calculating the peak of the best-fit cosine to the tuning curve. Spatiotemporal tuning was tested using gratings of varying SF [0.03–2 cycles per degree (cpd)] and TF [0.03–16 cycles per second (Hz)] moving in the preferred and antipreferred directions. Each sweep consisted of 4 s of motion in one direction, a 3-s pause, 4 s of motion in the opposite direction, followed by a 3-s pause. Firing rates were averaged over 3–5 sweeps.

Orthodromic stimulation

Neurons in the LM received orthodromic electrical stimulation with single shocks (0.5 ms, 25–400 μA, 0.3 Hz) that were delivered through a Teflon-coated stainless-steel bipolar stimulating electrode positioned in the area of the Wulst that contains LM-projecting neurons (12.5 mm anterior and 1.5 mm lateral from interaural zero, 1.5 mm ventral to the surface of the telencephalon; see following text, *Technical considerations*). The tips of the bipolar electrode were staggered by 0.5 mm. The constant-current pulses were produced by an S48 stimulator (Grass-Telefactor, West Warwick, RI) connected to a PSIU6 stimulus isolation unit (Grass-Telefactor). Note that the 0.5-ms single-shock pulse duration introduces a small measurement error (i.e., about 0.5 ms) because it is difficult to separate response latency from the pulse onset versus pulse offset.

Wulst inactivation general procedure

The procedure to measure the effects of Wulst inactivation was as follows. *1*) Based on stereotaxic coordinates, bone and dura overlaying the Wulst were removed, and the bipolar stimulating electrode and injecting pipette [about 25 μm tip diameter, filled with 4% lidocaine (Sigma-Aldrich, St. Louis, MO) in phosphate-buffered saline (pH = 7.4)] were positioned in the Wulst. The stimulating electrode was angled at 45° in the coronal plane and penetrated 1.5 mm into the surface of the telencephalon. The pipette, which was oriented vertically, was positioned based on trigonometric calculations so that the tip was located as close as possible to the 2 poles of the stimulating electrode. *2*) *Prelidocaine measures*: A recording microelectrode was lowered into the pretectum, and the direction and spatiotemporal tuning of an LM neuron was characterized (see *Visual stimulus presentation* above), as was the response to electrical stimulation of the Wulst (see *Orthodromic stimulation* above). *3*) Lidocaine was injected into the Wulst (2–4 μl) using a picospritzer (General Valve Corporation). Because the washout time of lidocaine is about 20 min (Sandkühler et al. 1987), supplemental injections of lidocaine were administered every 10 min to prolong the inactivation of the Wulst. *4*) *Postlidocaine measures:* Five minutes after the initial injection of lidocaine, the response properties of the LM neuron and the effects of Wulst electrical stimulation were tested again. *5*) *Recovery measures:* After the last application of the pharmacological blockade, lidocaine was allowed to wash out for 40–60 min, and the response properties of the LM neuron and the effects of electrical stimulation were tested a final time.

nBOR inactivation general procedure

The procedure to measure the effects of nBOR inactivation was as follows. *1*) The nBOR was located based on stereotaxic coordinates (Karten and Hodos 1967), and the dorsal border of the nBOR was determined with extracellular recording. *2*) The recording electrode was replaced with an injecting pipette filled with lidocaine (see *Wulst inactivation general procedure* above). The pipette was positioned such that the tip was at the approximate depth of the dorsal-most responsive nBOR cell from the recording track. *3*) A bipolar stimulating electrode was positioned in the Wulst (see *Wulst inactivation general procedure* above). *4*) A recording microelectrode was lowered into the pretectum, and the direction and spatiotemporal tuning of an LM neuron was characterized (see *Visual stimulus presentation* above), as was the response to electrical stimulation of the Wulst (see *Orthodromic stimulation* above). *5*) Lidocaine (0.25–0.5 μl) was injected into the nBOR (for details see *Wulst inactivation general procedure* above). *6*) Five minutes after the initial injection of lidocaine, the response properties of the LM neuron and the effects of Wulst electrical stimulation were tested again. *7*) After the last application of the pharmacological blockade, lidocaine was allowed to wash out for 40–60 min, and the response properties of the LM neuron and the effects of electrical stimulation were tested a final time.

Technical considerations

The hyperstriatum accessorium (HA) and hyperstriatum intercalatus superior (HIS) of the pigeon Wulst extend 14.5–7.5 mm anterior of interaural zero, and are ≤3–4 mm in the mediolateral and dorsoventral dimensions (Karten and Hodos 1967). The approximate volume of the HA and HIS combined is 40 mm^3. Injection of the retrograde tracer Cholera Toxin Subunit B into the LM revealed that

only a discrete population of neurons in the Wulst project to the pretectum (C. J. Ogilvie, N. A. Crowder, I. R. Winship, A. P. Nguyen, K. G. Todd, and D.R.W. Wylie, unpublished observations). The LM-projecting neurons form a dorsoventral strip located in the lateral margin of HA, along the boarder of HIS. In the rostrocaudal dimension, these cells extend from about 13.75 to 11.25 mm anterior to interaural zero. The approximate volume of the region containing the LM-projecting neurons is 10 mm^3.

The effective spread of 1 μl of lidocaine was investigated by Sandkühler et al. (1987) and Martin (1991), and was estimated to have a radius of 1.4–1.7 mm (which translates to a volume of 11.5–20.6 mm^3). Given that the effective spread of 1 μl of lidocaine is just enough to encompass the area of Wulst that projects to the LM, we are confident that 2–4 μl of lidocaine inactivated all afferents from the Wulst to LM.

Follett and Mann (1986) investigated the current spread of both monopolar and concentric bipolar electrodes. Extrapolating from the strength-spread and strength-duration curves provided by Follett and Mann (1986), we estimate that the effective current spread of a 400-μA pulse lasting 500 μs is $\geq$2 mm. Furthermore, stimulation intensities of 100–400 μA certainly provide enough current spread to include the area of Wulst that projects to the LM. Thus the extent of the lidocaine block and the electrical stimulation (which confirms the efficacy of the block) spread through a large portion of the Wulst, and certainly included the Wulst neurons that project to the LM.

Histology

In some cases, a dye spot was left at the final recording site by iontophoretically injecting the Pontamine sky blue and NaCl from the recording electrode (+3 μA, 3 s ON/3 s OFF, for 20 min). At the end of the recording session, the animals were given an overdose of sodium pentobarbitol (100 mg/kg) and immediately perfused with saline (0.9%) followed by paraformaldehyde [4% in 0.1 M phosphate buffer (PB), 4°C]. Brains were extracted, postfixed for 2–12 h (4% paraformaldehyde, 20% sucrose in 0.1 M PB), and cryoprotected in sucrose overnight (20% in 0.1 M PB). Frozen sections (45 μm thick in the coronal plane) through the LM, nBOR, and Wulst were collected. Sections were mounted onto gelatin chrome aluminum-coated slides and lightly counterstained with neutral red. The tissue was then examined using light microscopy to confirm the locations of electrode tracks and dye spots in the LM, and the stimulating electrode and lidocaine injecting pipette tracks in the Wulst.

RESULTS

We recorded from a total of 69 LM neurons in 12 pigeons. The directional and spatiotemporal properties of 45 LM neurons were quantitatively analyzed, whereas the directional preferences of 9 additional neurons were obtained from the handheld stimulus alone. Fifty-nine LM neurons were tested with orthodromic stimulation from the Wulst. Furthermore, the directional tuning and spatiotemporal response properties of 20 LM neurons were tested before, during, and after the Wulst was inactivated with lidocaine. Histological analysis revealed that the stimulating electrode and lidocaine injecting pipette were in the desired position in the Wulst. Dye spots and electrode tracks were seen in the lateral and medial subnuclei of LM (LMl and LMm, respectively; Gamlin and Cohen 1988b).

Normal properties of LM neurons

All 45 LM neurons that were quantitatively examined for directional tuning exhibited direction selectivity. A unit was assigned a direction preference by calculating the maximum of the best cosine fit to the tuning curve. Twenty, 4, 5, and 16 LM neurons preferred forward (i.e., temporal to nasal), downward, backward, and upward motion, respectively. Of the 9 LM neurons tested with the handheld stimulus, 2, 4, 2, and 1, preferred forward, downward, backward, and upward motion, respectively. The predominance of neurons preferring forward motion is consistent with previous studies of the pigeon LM (Crowder et al. 2003; Winterson and Brauth 1985; Wylie and Crowder 2000; Wylie and Frost 1996).

The spatiotemporal response properties of the 45 neurons were also quantitatively examined. Using *SigmaPlot*, contour plots were constructed where TF was on the ordinate, SF was on the abscissa, and the mean firing rate relative to the spontaneous firing rate (SR) was plotted on the *z*-axis. Given that motion in the preferred and antipreferred directions generally results in excitation and inhibition of the neuronal firing, respectively, we refer to excitatory response (ER) and inhibitory response (IR) plots (e.g., Figs. 5 and 7). The location of the peak in the contour plots was assigned quantitatively by fitting the primary peak in each contour plot to a 2-dimensional Gaussian function (Crowder et al. 2003; Perrone and Thiele 2001). Consistent with previous studies of the pretectum (Crowder et al. 2003; Ibbotson et al. 1994; Wylie and Crowder 2000), the peaks cluster into 2 quadrants: cells responding best to gratings of low SF/high TF (29 cells), or high SF/low TF (16 cells). Following Ibbotson et al. (1994), we refer to these as "fast" and "slow" cells, respectively.

Orthodromic Wulst stimulation

All 59 LM neurons that were tested with orthodromic stimulation of the Wulst showed a modulation in firing. The average stimulation threshold to elicit modulation was 65 μA (SD = 38 μA). Two distinct effects were observed after Wulst stimulation. One group of cells showed a short-latency excitation followed by longer-latency inhibition. The second group of cells showed only the longer-latency inhibition. We refer to these groups as W+ cells and W− cells, respectively. Figure 1 shows data from a W+ cell, including the average spike waveform (Fig. 1*A*), the effects of subthreshold (Fig. 1*B*; 25 μA), and suprathreshold stimulation (Fig. 1, *C* and *D*; 200 μA). Suprathreshold stimulation of the Wulst elicited a burst of 3–5 spikes at an average first-spike latency of 20 ms (SD = 1.6 ms). As expected with orthodromic stimulation, the average first-spike latency decreased as the current intensity increased (in this case from 21 $\pm$ 2.3 ms at 50 μA to 20 $\pm$ 1.6 ms at 200 μA). As shown in Fig. 1*D*, the excitatory burst was followed by a period of inhibition (at about 40–90 ms). At higher intensities, the effects of the stimulation were often manifested as oscillations between excitation and inhibition lasting up to 1 s (Fig. 1*D*). The consistency of the stimulation effect is shown in the raster plot and PSTH (Fig. 1*D*).

Figure 2 shows raster plots and PSTHs illustrating the effects of stimulation of the Wulst for a W+ (Fig. 2*A*) and W− cell (Fig. 2*B*). We used 5-ms bins for the PSTHs because interspike-interval analysis revealed that most LM neurons have an interspike interval >5 ms (average = 7.2ms, SD = 3.7 ms). Figure 2*A* shows PSTHs of the response of a W+ neuron to varying stimulation intensities (50, 100, 200 μA). When the Wulst was stimulated with 200-μA pulses, there was a short-

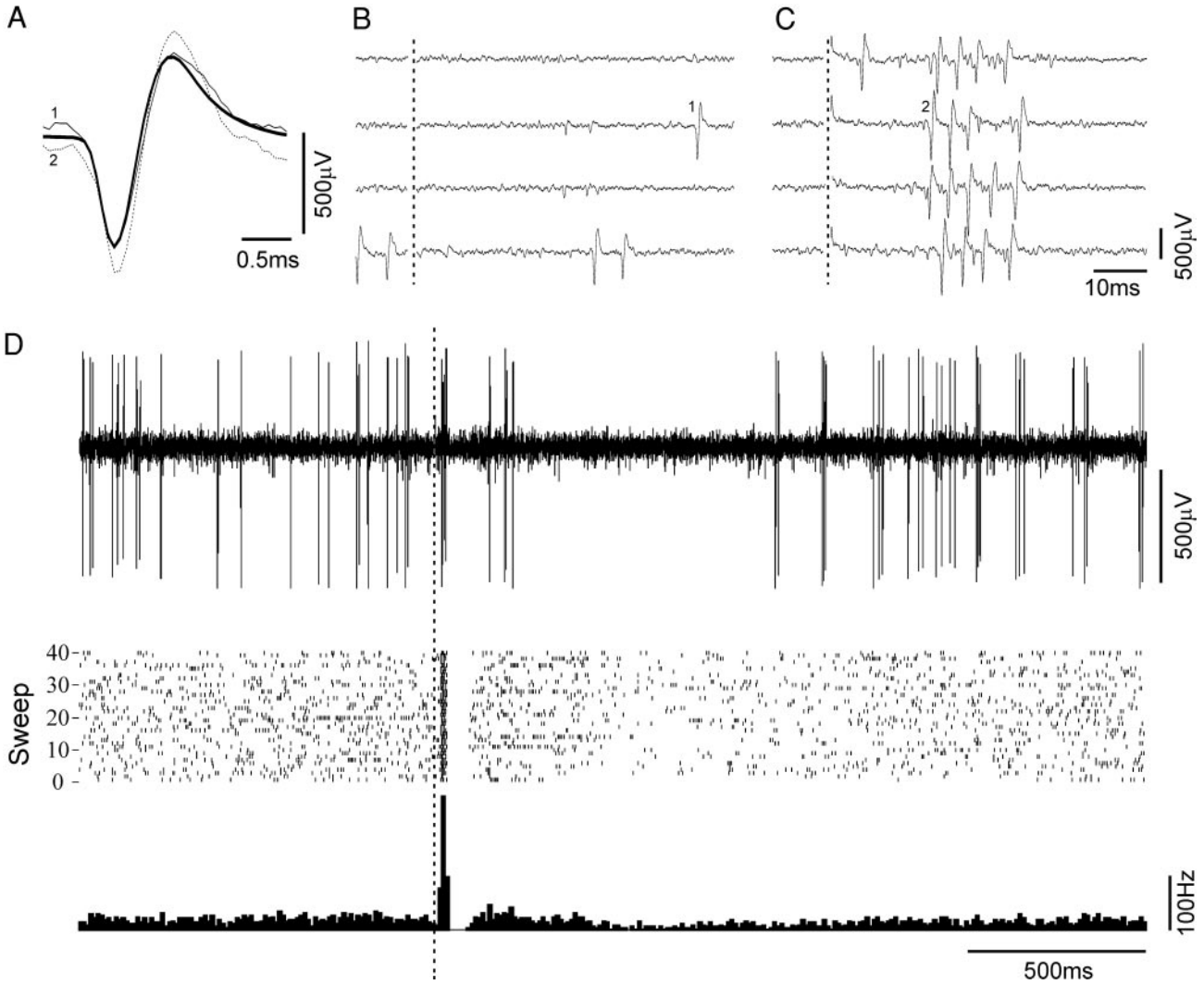

FIG. 1. Raw traces, raster plot, and peristimulus time histograms (PSTHs) illustrating the effect of electrical stimulation of the Wulst on a W+ neuron in the lentiformis mesencephali (LM). *A*: average waveform of the LM unit (thick line). Superimposed are two raw traces denoted by Arabic numerals and representing individual spikes as shown in *B* and *C*. Effects of subthreshold (25 μA) and suprathreshold (200 μA) electrical stimulation are shown in raw form for 4 separate raw sweeps in *B* and *C*, respectively. Dotted vertical lines indicate the time of stimulation (stimulus artifact cropped). *D*: stimulation effect on a longer time scale. *Top panel*: raw trace shows a single stimulation trial from the raster sweep and PSTH (*middle* and *bottom panels*, respectively). A prominent excitation/inhibition sequence can be observed in this neuron.

latency excitation (beginning at about 10 ms) followed by inhibition at a latency of about 50 ms and a smaller excitatory period at a latency of about 110 ms. At 100 μA, the short-latency excitation was less marked, as was the rebound inhibition. Stimulation at 50 μA failed to elicit any stimulation effect. The neuron in Fig. 2*B* showed inhibition only after Wulst stimulation (i.e., a W− neuron), but showed a similar progression of stimulation effects with varying stimulation intensities. At 200 μA this neuron showed inhibition at a latency of about 25 ms, followed by excitation at a latency of about 150 ms. This pattern was less pronounced at 100 μA and absent at 50 μA.

Stimulation effects were quantitatively analyzed by converting every 5-ms bin in the PSTH of an LM neuron into z-scores. Trials using subthreshold or no stimulation were used to calculate the average spontaneous rate of the neuron, and were compared with the results for suprathreshold stimulation intensity of 200 μA. Deviations from the spontaneous rate were not considered significant unless they exceeded a z-score of 2. The stimulation latencies for W+ and W− neurons were 13.5 ± 5 and 28.3 ± 8 ms, respectively (mean ± SD). These latencies were significantly different (single-sample Student *t*-test, $P < 0.0000001$). The rebound inhibition exhibited by W+ neurons occurred significantly later (35 ± 7 ms; single-sample Student *t*-test, $P < 0.004$) than the initial inhibitory effect of W− neurons. It is likely that the inhibition shown by W+ and W− neurons occurs at a similar latency, but the true latency of W+ inhibition is masked by the excitatory burst that precedes it. Of the 59 LM neurons tested, 34 (58%) were W+ cells and 25 (42%) were W− cells.

Directional tuning, as determined by best fit to cosines, for 27 W+ and 18 W− neurons is shown in Fig. 3, *A* and *B*, respectively. The orientation of each line represents the direction preference of individual W+ (Fig. 3*A*) and W− (Fig. 3*B*) neurons. From this figure it is clear that there were no differences between W+ and W− cells with respect to their direc-

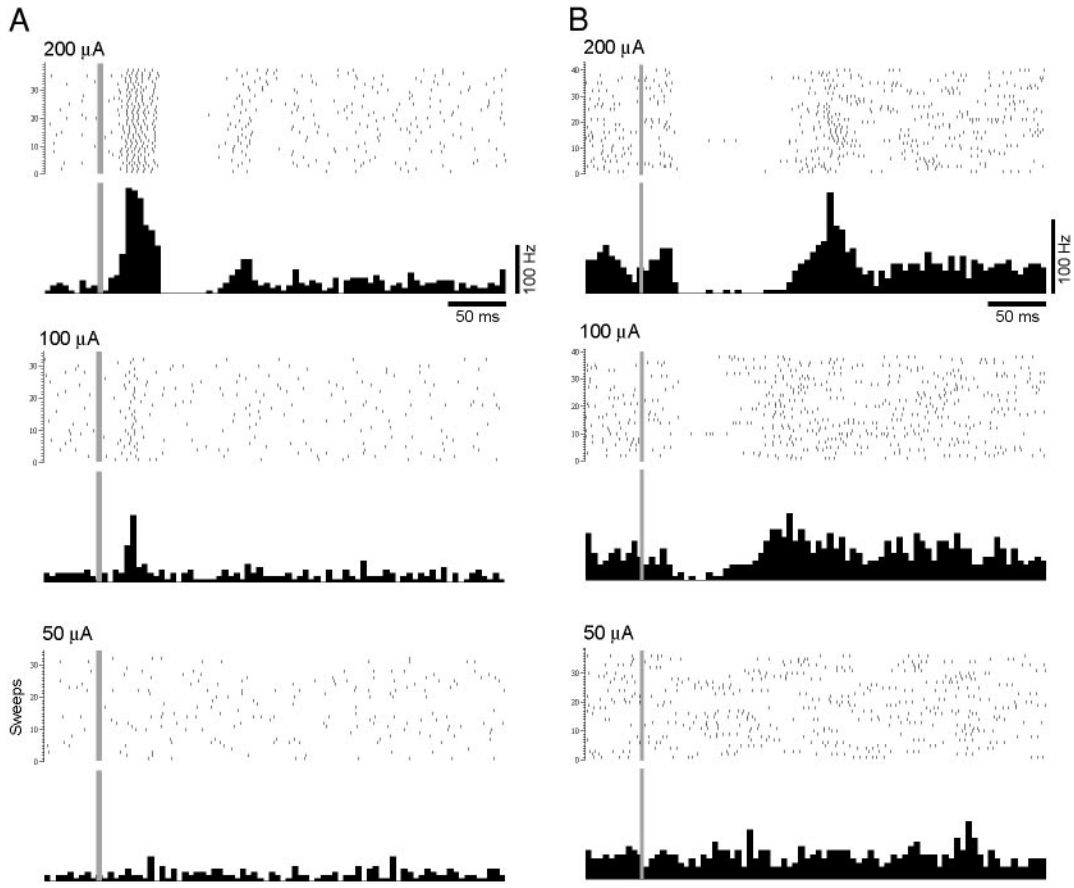

FIG. 2. Raster plots and PSTHs illustrating the effects of electrical stimulation of the Wulst on neurons in the LM. *A* and *B*: effects of 50-, 100-, and 200-μA Wulst stimulation on a W+ and W− neuron, respectively. Gray bars indicate the time of the stimulation artifact.

tion preferences. Figure 3*C* plots the locations of the primary ER peaks from the spatiotemporal contour plots of 27 W+ (empty circles) and 17 W− neurons (filled circles). Of the W+ cells, 18 were fast cells, and 9 were slow cells. Of the W− neurons, 11 were fast cells and 6 were slow cells. From Fig. 3*C* it is clear that there were no differences between W+ and W− cells with respect to their spatiotemporal tuning.

Effects of Wulst inactivation

The directional tuning and spatiotemporal response properties of 20 LM neurons were tested before, during, and after the Wulst was inactivated with lidocaine. The Wulst was inactivated for ≤1 h using multiple lidocaine injections (see METHODS). Of these 20 neurons, 13 were also tested with orthodromic stimulation from the Wulst before, during, and after the Wulst was inactivated with lidocaine. In all cases, Wulst inactivation completely eliminated all electrical stimulation effects. Moreover, full recovery of the stimulation effects was seen for every cell after the lidocaine was allowed to wash out. Figure 4 shows a W+ neuron before the Wulst was injected with lidocaine (Fig. 4*A*), a few minutes after the lidocaine injection (Fig. 4*B*), and after the lidocaine effect had washed out (Fig. 4*C*). This explicit reversible inactivation effect was evident for all 13 LM neurons that were tested with Wulst electrical stimulation.

CHANGES IN SPONTANEOUS RATE OF LM NEURONS AFTER WULST INACTIVATION. The spontaneous rate was calculated pre- and postlidocaine by averaging across at least ten 4-s epochs. The average SR across all 20 LM neurons before Wulst inactivation was 27.3 ± 12.7 spikes/s (mean ± SD). For individual neurons, changes in the SR of LM neurons after Wulst inactivation were calculated as percentage difference (for decreases, %change = {[postlidocaine − prelidocaine]/prelidocaine} × 100; for increases, =[postlidocaine − prelidocaine]/postlidocaine} × 100). In 5 cases there was a significant decrease in SR (21–66%), whereas 2 cases showed a significant increase (23 and 35%) (*t*-test, $P < 0.0025$; Bonferroni correction for multiple comparisons), and 13 cases showed no significant change. The average change in SR across all 20 cases was −7.9%.

EFFECTS OF WULST INACTIVATION ON THE DIRECTION TUNING OF LM NEURONS. None of the LM neurons showed a significant change in direction preference after Wulst inactivation. Two neurons showed changes of 14 and 16°, whereas the direction change for other neurons did not exceed 6° (mean = 2.5°). The magnitude of modulation, both excitation and inhibition, remained unchanged for all neurons. Figure 5*A* shows the direction tuning of an LM neuron before (solid) and after (dashed) Wulst inactivation.

SPATIOTEMPORAL CHANGES AFTER WULST INACTIVATION. The spatiotemporal properties of all 20 LM neurons were examined before and during Wulst inactivation, and for 16 neurons after

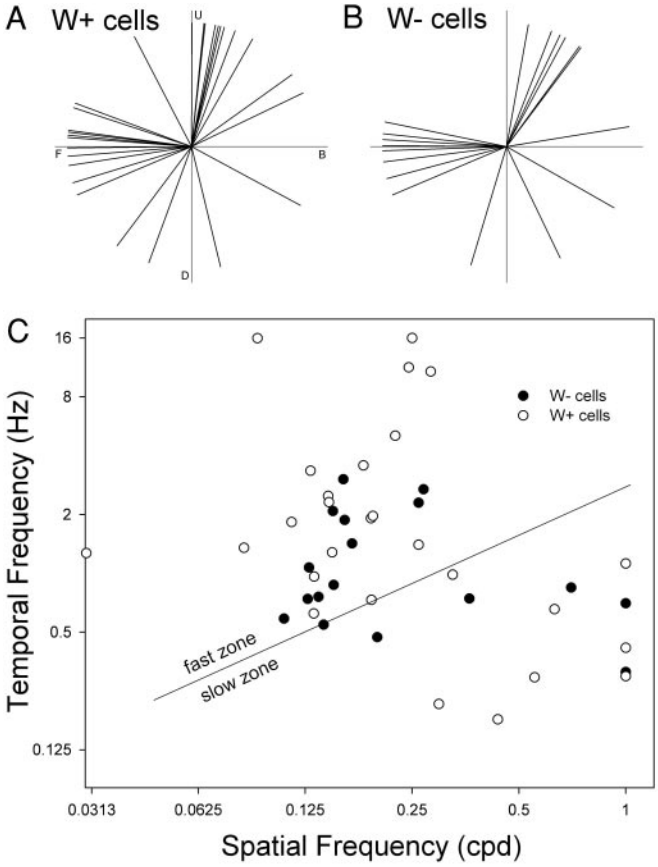

FIG. 3. Directional and spatiotemporal tuning of LM neurons. Preferred directions for W+ and W− neurons, as calculated from the peak of the best-fit cosine to the direction-tuning curve are shown in *A* and *B*, respectively. U, B, D, and F: up, back (nasal to temporal), down, and forward (temporal to nasal) motion. *C*: locations of the primary peaks from the excitatory response (ER) contour plots for W− and W+ neurons are shown as filled and empty dots, respectively. The diagonal line represents a stimulus velocity of 4°/s, which Ibbotson and Price (2001) used to distinguish the "fast" and "slow" groups in both the wallaby NOT and the pigeon LM.

lidocaine washout. Inactivation of the Wulst did not significantly affect the spatiotemporal profiles of any LM neurons tested. Figure 5*B* shows the ER and IR plots of a single LM neuron before (Fig. 5*B*, *left*) and during (Fig. 5*B*, *right*) Wulst inactivation. In these plots excitatory peaks are shown in white and inhibitory peaks are shown in black. For the cell shown in Fig. 5*B*, both the ER plot prelidocaine (Fig. 5*B*, *top left*) and ER plot postlidocaine (Fig. 5*B*, *top right*) had a main peak at 1 cpd/0.5 Hz (+50 spikes/s), and a smaller peak at 0.06 cpd/16 Hz (30 spikes/s). Similarly, the IR plot prelidocaine (Fig. 5*B*, *bottom left*) and postlidocaine (Fig. 5*B*, *bottom right*) looked very similar, with a single inhibitory peak at 1 cpd/0.5 Hz (−16 spikes/s).

Effects of nBOR inactivation on the response properties of LM neurons

There is a reciprocal connection between the LM and nBOR (Azevedo et al. 1983; Brecha et al. 1980; Wylie et al. 1997). Because the Wulst also projects to the nBOR (Rio et al. 1983), we hypothesized that the longer-latency modulation of LM cells that resulted from Wulst stimulation might arise from the nBOR cells that are also activated by Wulst stimulation. To test this possibility, the effect of Wulst electrical stimulation on 4 LM neurons was measured before, during, and after the nBOR was inactivated with lidocaine. The direction and spatiotemporal response properties of these LM neurons were also measured during nBOR inactivation, serving to replicate the data presented by Crowder et al. (2003), and confirm inactivation of the nBOR.

Figure 6 shows PSTHs from a W− neuron before the nBOR was injected with lidocaine (Fig. 6*A*), a few minutes after the lidocaine injection (Fig. 6*B*), and after the lidocaine washed out (Fig. 6*C*). Before nBOR inactivation, and after the lidocaine washout period, the W− neuron showed long-latency inhibition starting at 20 ms. When the nBOR was inactivated, this inhibition was strongly diminished. This decrease in long-latency inhibition was evident in 2 W+ cells and one W− cell. The remaining neuron was a W− cell that showed a lengthening in the duration of its long-latency inhibition (20–130 ms prelidocaine; 20–180 ms during lidocaine). The short-latency excitation shown by W+ cells was not affected by nBOR inactivation (not shown).

Figure 7*A* shows the effect of nBOR inactivation on the ER plot of an LM neuron. Prelidocaine, the ER plot showed two excitatory peaks (primary, 0.25 cpd/0.5 Hz; secondary, 0.25 cpd/8 Hz). Both peaks diminished in size during nBOR inactivation, but returned after lidocaine washout. Generally, ER plots showed less excitation to low SF/high TF stimuli (3 of 4 cells) and more excitation to high SF/low TF

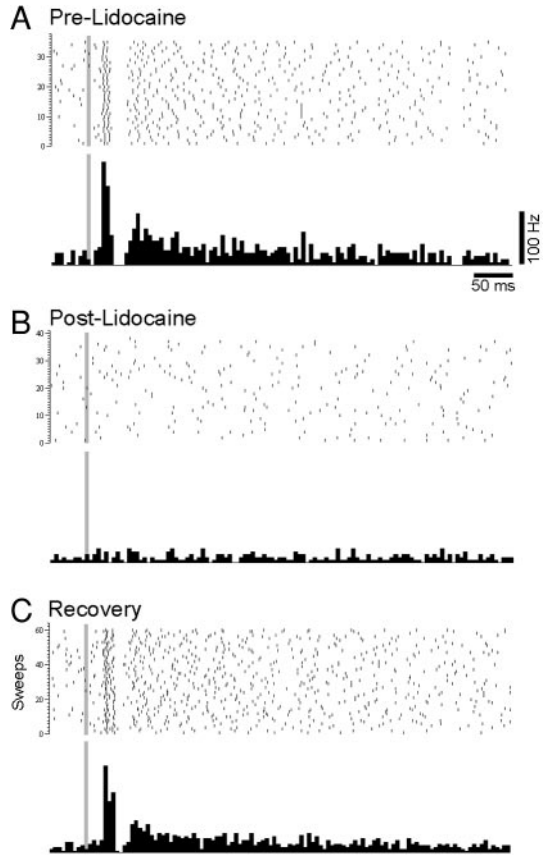

FIG. 4. Effects of Wulst inactivation on stimulation effects. Raster plots and peristimulus time histograms illustrating the effects of Wulst electrical stimulation on a W+ neuron before the Wulst was injected with lidocaine (*A*), a few minutes after the lidocaine injection (*B*), and after the lidocaine has washed out (*C*). Gray bars indicate the time of the stimulation artifact.

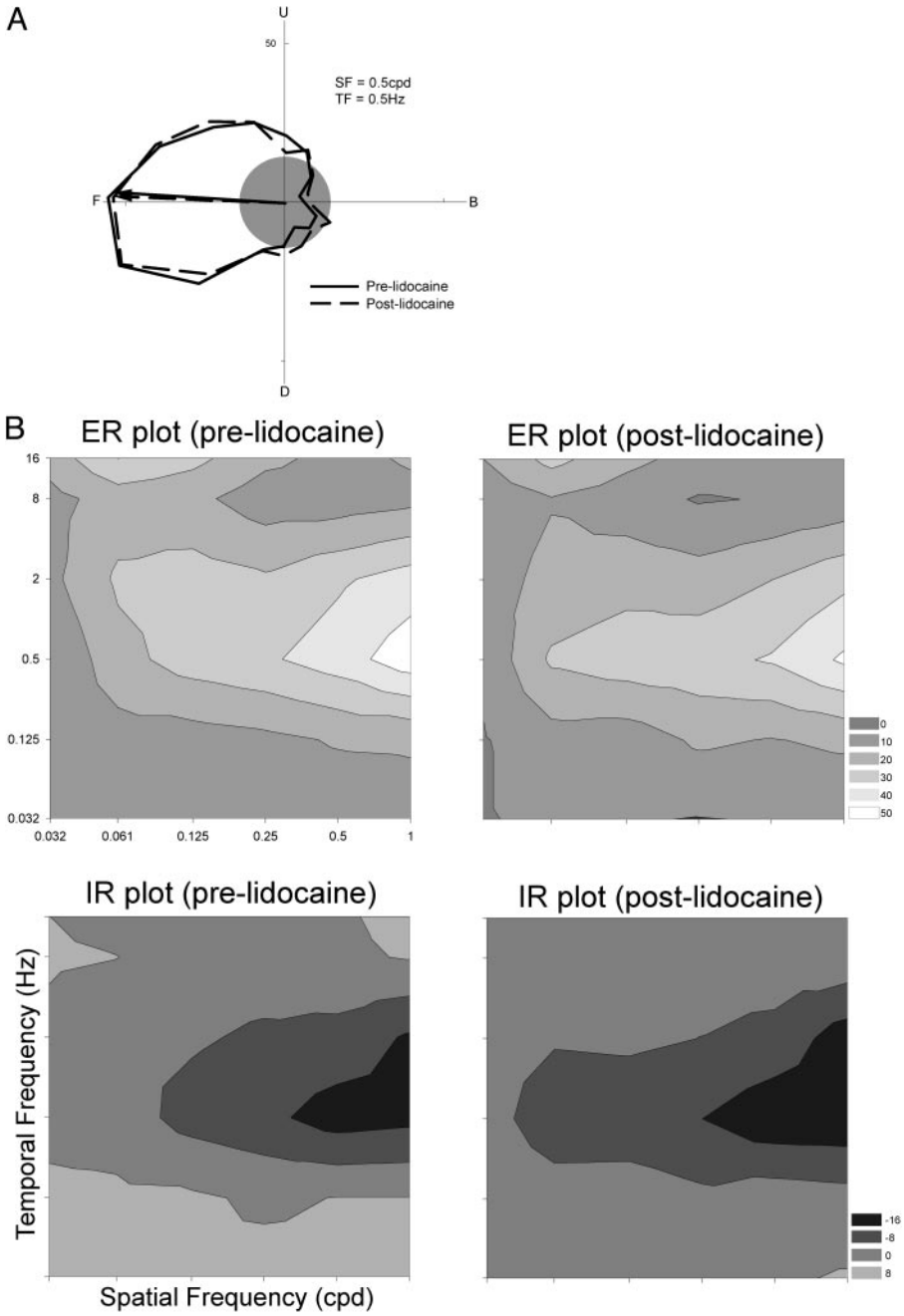

FIG. 5. Effects of visual Wulst inactivation on the directional and spatiotemporal tuning of an LM neuron. *A*: polar plot illustrating the directional tuning of an LM neuron before (solid lines) and after (dashed lines) the Wulst was injected with lidocaine. Firing rate (spikes/s) relative to the spontaneous rate (SR; gray circle) is plotted as a function of the direction of motion in polar coordinates (i.e., the SR was set to zero; outside the gray circle = excitation, inside = inhibition). Solid and dashed arrows represent the neuron's preferred direction prelidocaine and postlidocaine, respectively. U, B, D, and F: up, back (nasal to temporal), down, and forward (temporal to nasal) motion. Temporal and spatial frequency (TF, SF) used to collect the directional tuning is indicated. *B*: contour plots of the responses to gratings of varying SF and TF drifting in the preferred direction (ER plots) and antipreferred direction (IR plots). SF and TF are plotted on the abscissa and ordinate, respectively. Prelidocaine plots are shown on the *left*, and postlidocaine plots are shown on the *right*. Prelidocaine and postlidocaine contour plots use a common scale to represent the firing rate (spikes/s) above (+; white) or below (−; black) the spontaneous rate.

stimuli (all cells) moving in the preferred direction after nBOR inactivation. Figure 7*B* shows the effect of nBOR inactivation on the IR plot of another LM neuron. Prelidocaine, the IR plot showed one main inhibitory peak (1 cpd/0.5 Hz), which completely disappeared during nBOR inactivation and returned after lidocaine washout. The majority of IR plots (3 of 4 cells) showed less inhibition to high SF/low TF stimuli moving in the antipreferred direction. Figure 7*C* shows the effect of nBOR inactivation on the direction tuning of an LM neuron that preferred forward motion. Note that preferred direction for this neuron is not directly opposite the antipreferred direction. During nBOR

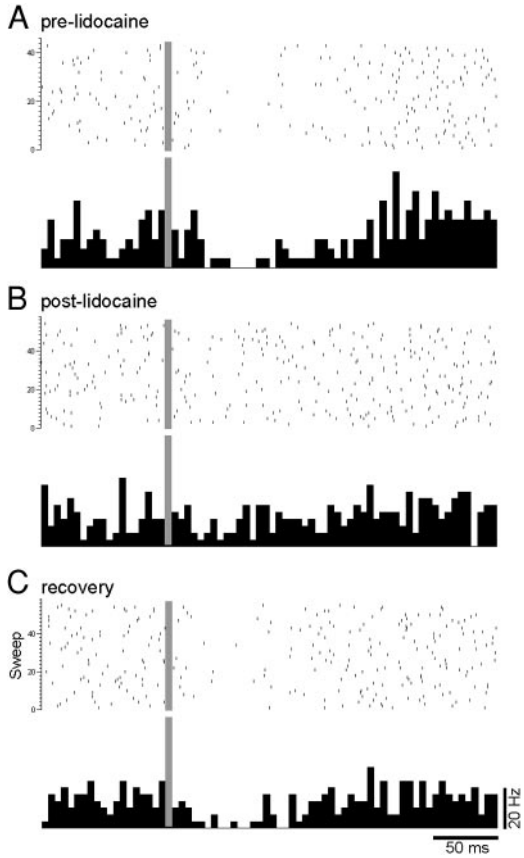

FIG. 6. Effects of inactivation of the nucleus of the basal optic root (nBOR) on Wulst stimulation effects. Raster plots and PSTHs illustrating the effects of Wulst electrical stimulation on a W− neuron before the nBOR was injected with lidocaine (*A*), a few minutes after the nBOR injection (*B*), and after the lidocaine has washed out (*C*). Gray bars indicate the time of the stimulation artifact.

inactivation this neuron showed no changes in its preferred direction, although there is more excitation to motion in the preferred direction and less inhibition to motion in the antipreferred direction. One other neuron showed this same pattern, whereas the depth of tuning for the remaining 2 neurons was not affected. None of the neurons showed changes in their preferred direction after nBOR inactivation.

DISCUSSION

In the present study we investigated the function of the projection from the Wulst to the pretectum (Gottlieb and McKenna 1986; Miceli et al. 1979). We electrically stimulated the Wulst and found that LM neurons were either excited (W+ cells) or inhibited (W− cells). However, when the Wulst was temporarily inactivated by lidocaine neither the directional nor spatiotemporal response properties of LM neurons were affected.

W+ and W− cells in the LM

This study is the first to demonstrate the effects of Wulst stimulation on the activity of pretectal neurons. Just over half of the LM neurons tested showed short-latency (13.5 ms) excitation to Wulst stimulation, whereas the remainder showed longer-latency (28.3 ms) inhibition to Wulst stimulation. We refer to these LM neurons as W+ cells and W− cells, respectively. Wulst stimulation effects did not appear to correlate with directional or spatiotemporal tuning. The bimodal distribution of latencies for W+ and W− neurons suggests a direct and indirect route from the Wulst to the LM. The short-latency excitatory stimulation effects seen in LM W+ neurons likely arise from the monosynaptic inputs they receive from the Wulst (Gottlieb and McKenna 1986; Miceli et al. 1979; Rio et al. 1983). Longer-latency inhibitory effects could be the result of polysynaptic feed-forward or even feed-back circuits within the LM itself or the result of feed-forward inhibitory projections from other pretectal nuclei also receiving Wulst input (see following text).

W+ and W− cells in the nBOR

Nogueira and Britto (1991) examined the effects of Wulst stimulation on the firing rate of nBOR neurons. Their findings were strikingly similar to those of the present study: nBOR neurons showed either a short-latency excitation (26%; average latency = 13 ms) or a longer-latency inhibition (38%; average latency = 35 ms). Clearly the nBOR has counterparts to the W+ (average latency = 13.5 ms) and W− (average latency = 28.3 ms) LM cells described in the present study. This argues for a similar function of the telencephalic projection to the pretectum and AOS.

Longer-latency modulation of LM neurons from Wulst stimulation: Wulst, LM, nBOR interactions

The initial longer-latency inhibition of the W− cells in response to Wulst stimulation, as well as the longer-lasting inhibitory/excitatory oscillations seen in both W+ and W− neurons, could arise from inhibitory interneurons in the pretectum and/or from Wulst stimulation following an indirect route through the nBOR (Brecha et al. 1980; Clarke 1977; Gamlin and Cohen 1988b; Wylie et al. 1997). When we inactivated nBOR, the long-latency modulation in response to Wulst stimulation was clearly affected. For 3 of 4 cases, there was a reduction in long-latency inhibition, and in one case there was an increase. It has been suggested that the projection from the nBOR to LM is predominantly inhibitory (Baldo and Britto 1990; van der Togt and Schmidt 1994), but also excitatory (Baldo and Britto 1990; Crowder et al. 2003). Oscillations seen in some LM neurons after electrical stimulation are likely attributable to the delicate balance in reciprocating activity between the nBOR and LM. Nogueira and Britto (1991), who examined the effects of Wulst stimulation on the activity of nBOR neurons (see above), came to an identical conclusion. They suggest that short-latency stimulation effects arise from direct Wulst input to the nBOR, whereas the longer-latency effects result from stimulation of the LM, which projects to the nBOR.

Function of the Wulst projection to the LM

Neurons in the LM show clear directional tuning (Fan et al. 1995; Fite et al. 1989; Katte and Hoffmann 1980; McKenna and Wallman 1985b; Winterson and Brauth 1985; Wylie and Crowder 2000; Wylie and Frost 1996) and are also tuned in the spatiotemporal domain (Ibbotson and Price 2001; Wylie and Crowder 2000). Furthermore, it has been shown that input from the nBOR affects the spatiotemporal tuning (but not direction

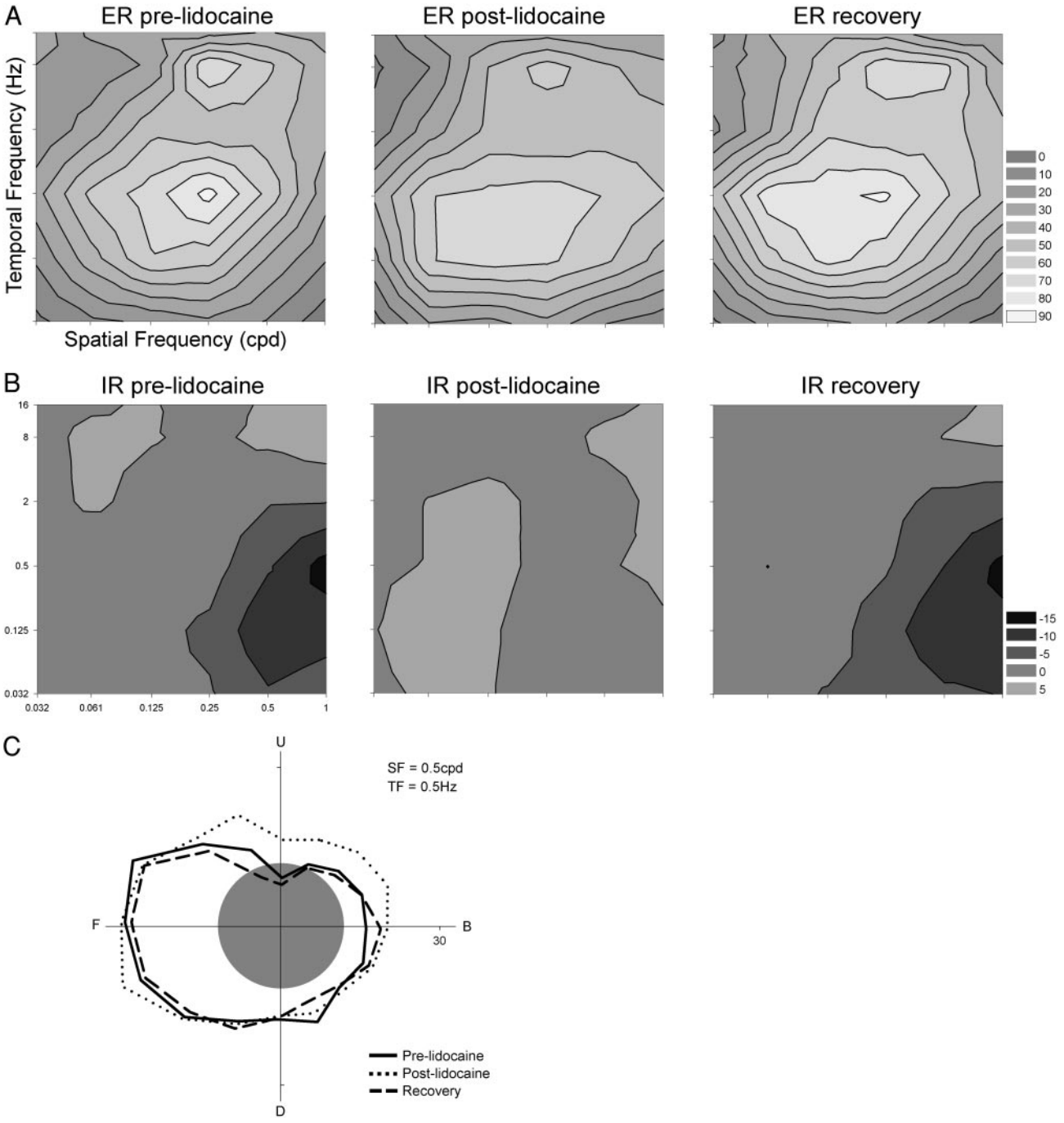

FIG. 7. Effects of inactivation of the nBOR on the directional and spatiotemporal tuning of neurons in the LM. Spatiotemporal tuning of LM neurons to gratings drifting in the preferred (ER plot, *A*) and antipreferred directions (IR plot, *B*) before, during, and after the nBOR was inactivated with lidocaine (prelidociane, postlidocaine, recovery). *C*: a polar plot indicating the direction tuning of an LM neuron before (solid), during (dotted), and after (dashed) nBOR inactivation. See caption to Fig. 5 for additional details.

preference) of LM neurons (Crowder et al. 2003). In addition to the nBOR, the Wulst represents another prominent source of extraretinal input to the LM. In this study, the Wulst was temporally inactivated with lidocaine to determine the function of the projection from Wulst to LM. Although Wulst inactivation altered the spontaneous rate of some LM neurons, it had no effect on the directional or spatiotemporal tuning of LM neurons. Despite the fact that we have negative findings in this regard, we have a very clear positive control: in every case where electrical stimulation was used (and as shown in Fig. 4), lidocaine injection did inactivate the input from the Wulst to the LM.

In a pair of studies investigating the function of the projection from the Wulst to the nBOR, Britto and colleagues (Britto et al. 1990; Hamassaki et al. 1988) argued that the Wulst contributes to the directional tuning of nBOR neurons. They compared the distribution of preferred directions in normal pigeons versus those that had the Wulst removed by aspiration.

They observed that the proportion of neurons preferring upward motion was reduced and the proportion of neurons preferring temporal-to-nasal motion was increased in the group with Wulst lesions. Given the results of the present study, these previous findings are difficult to reconcile. One could conclude that the Wulst contributes to directional tuning of nBOR neurons, but not LM neurons. However, this explanation is unsatisfactory because the electrical stimulation of the Wulst results in similar modulation of nBOR and LM units (Nogueira and Britto 1991; present study). We suggest that there is an inherent problem with the between-groups design used by Hamassaki et al. (1988) and Britto et al. (1990) insofar as the differences observed could represent a sampling bias. In fact, their control groups suggest that perhaps this is the case. From Fig. 2 of Britto et al. (1990), most of the nBOR neurons in the control group preferred upward or downward motion, but neurons preferring nasal-to-temporal motion were absent. However, 3 different labs have found that nBOR in normal pigeons contains equal proportions of neurons preferring upward, downward, and nasal-to-temporal motion (Gioanni et al. 1984; Wylie and Frost 1990; Zhang et al. 1999; see also Rosenberg and Ariel 1990). This possible sampling bias is not an issue in within-subject designs such as reversible inactivation studies. It is likely that this issue will not be resolved until the reversible inactivation methods used in the present study are applied to the nBOR. Under these circumstances, visual response properties of single nBOR units could be tested before and after the inactivation of the Wulst. Indeed, Nogueira and Britto (1991) themselves stated that reversible inactivation studies are needed to precisely evaluate the effect of visual Wulst on nBOR neurons.

If the Wulst does not contribute to the directional or spatiotemporal tuning of LM neurons, what is the function of this projection? The Wulst is considered to be a homolog of mammalian primary visual cortex based on embryological, histochemical, and physiological characteristics (Karten and Shimizu 1989; Karten et al. 1973; Medina and Reiner 2000). This excludes the rostral tip of the Wulst, which is somatosensory (Medina and Reiner 2000; Wild 1987). Like V1, neurons in the visual Wulst have small receptive fields and are thought to be involved in form vision. Many respond to small moving stimuli, and there is evidence of orientation tuning, binocularity, and columnar organization (Liu and Pettigrew 2003; Miceli et al. 1979; Pettigrew and Konishi 1976; Revzin 1969; Wilson 1980). In owls, the visual Wulst appears to play a major role in the processing of binocular vision and higher-level visual stimuli such as subjective contours (Neider and Wagner 1999; Pettigrew 1979; Porciatti et al. 1990). However, even large lesions to the Wulst produce surprisingly few visual deficits in pigeons (e.g., Hodos et al. 1984; Pritz et al. 1970; Riley et al. 1980). If the LM-projecting neurons in the Wulst are involved in form vision, it is possible that the projection from the Wulst to the pretectum and AOS is to adjust the gain of a subset of optic flow sensitive neurons when the animal is attending to small objectlike stimuli.

It is also possible that the Wulst neurons that project to the LM are somatosensory or somatosensory/visual neurons. First, Deng and Wang (1992, 1993) demonstrated that there is significant overlap between areas of the Wulst that process visual and somatosensory information, with some neurons even responding to both visual and somatosensory stimuli (also see Medina and Reiner 2000). Second, from our own observations, the area of the Wulst containing the LM-projecting neurons does overlap with the area in which somatosensory responses are evoked (Deng and Wang 1992, 1993; Wild 1987). Somatosensory information such as air passing through the pigeon's feathers could be used in addition to optic flow information to analyze self-motion. In support of this idea, neurons classified as bimodal (visual and somatosensory) as well as trimodal (visual, somatosensory, and vestibular) have been found in the ventral intraparietal area (VIP) of macaque monkeys, which along with the middle superior temporal area (MST) is responsible for the cortical processing of optic flow in primates (Bremmer et al. 2000). These ideas suggest that perhaps LM neurons are modulated by somatosensory stimulation and that inactivation of the Wulst would block this modulation.

Function of the telencephalic input to the pretecum and AOS in mammals

The presence of a telencephalic projection on the AOS and pretectum appears to be highly variable among both lateral-eyed and frontal-eyed species. For example, the pretectum receives cortical afferents in frontal-eyed species such as cats and monkeys (Hoffmann et al. 1991; Ilg and Hoffmann 1993; Mustari et al. 1994; Schoppmann 1981), but not opossums (Pereira et al. 2000). In lateral-eyed animals, the NOT receives cortical input in rats (Shintani et al. 1999), guinea pigs (Lui et al. 1994), and rabbits (Hollander et al. 1979), but not in hamsters (Lent 1982) or tree shrews (Huerta et al. 1985). Electrophysiological, behavioral, and developmental studies in cats have suggested that the cortical projection to the AOS and pretectum alters the gain asymmetries of vertical and horizontal optokinetic nystagmus as an adaptation to frontal eye placement (Grasse and Cynader 1986, 1987, 1988, 1990). Because the pigeon is a lateral-eyed animal, and the telencephalic inputs to the LM do not affect the directional tuning of these neurons, this projection likely serves a different purpose than in the cat.

GRANTS

This research was supported by grants from the Natural Sciences and Engineering Research Council (NSERC) of Canada to D.R.W. Wylie and C. T. Dickson. D.R.W. Wylie was supported by the Canada Research Chairs Program (Tier II). C. T. Dickson was supported by the Alberta Heritage Foundation for Medical Research (AHFMR) Scholars Program and N. A. Crowder was supported by a Julie Payette NSERC postgraduate scholarship.

Present address of N. A. Crowder: Australian National University Visual Sciences Group, Research School of Biological Sciences, Canberra ACT 2601, Australia.

REFERENCES

Azevedo TA, Cukiert A, and Britto LRG. A pretectal projection upon the accessory optic nucleus in the pigeon: an anatomical and electrophysiological study. *Neurosci Lett* 43: 13–18, 1983.

Baldo MV and Britto LR. Accessory optic-pretectal interactions in the pigeon. *Braz J Med Biol Res* 23: 1037–1040, 1990.

Berson DM and Graybiel AM. Some cortical and subcortical fiber projections to the accessory optic nuclei in the cat. *Neuroscience* 5: 2203–2217, 1980.

Blanks RH, Giolli RA, and Pham SV. Projections of the medial terminal nucleus of the accessory optic system upon pretectal nuclei in the pigmented rat. *Exp Brain Res* 48: 228–237, 1982.

Brecha N, Karten HJ, and Hunt SP. Projections of the nucleus of basal optic root in the pigeon: an autoradiographic and horseradish peroxidase study. *J Comp Neurol* 189: 615–670, 1980.

Bremmer F, Duhamel JR, Hamed SB, and Graf W. Stages of self-motion processing in primate posterior parietal cotex. *Int Rev Neurobiol* 44: 173–198, 2000.

Britto LR, Gasparotto OC, and Hamassaki DE. Visual telencephalon modulates directional selectivity of accessory optic neurons in pigeons. *Vis Neurosci* 4: 3–10, 1990.

Burns S and Wallman J. Relation of single unit properties to the occulomotor function of the nucleus of the basal optic root (AOS) in chickens. *Exp Brain Res* 42: 171–180, 1981.

Carpenter RHS. *Movement of the Eyes.* London: Pion, 1977.

Clark PGH. Some visual and other connections to the cerebellum of the pigeon. *J Physiol* 243: 267–285, 1977.

Collewijn H. Direction-selective units in the rabbit's nucleus of the optic tract. *Brain Res* 100: 489–508, 1975a.

Collewijn H. Oculomotor areas in the rabbit's midbrain and pretectum. *J Neurobiol* 6: 3–22, 1975b.

Crowder NA, Dawson MRW, and Wylie DRW. Temporal frequency and velocity-like tuning in the pigeon accessory optic system. *J Neurophysiol* 90: 1829–1841, 2003.

Crowder NA, Lehmann H, Parent MB, and Wylie DR. The accessory optic system contributes to the spatio-temporal tuning of motion-sensitive pretectal neurons. *J Neurophysiol* 90: 1140–1151, 2003.

Crowder NA and Wylie DR. Fast and slow neurons in the nucleus of the basal optic root in pigeons. *Neurosci Lett* 304: 133–136, 2001.

Deng C and Wang B. Overlap of somatic and visual response areas in the Wulst of pigeon. *Brain Res* 582: 320–322, 1992.

Deng C and Wang B. Convergence of somatic and visual afferent impulses in the Wulst of pigeon. *Exp Brain Res* 96: 287–290, 1993.

Distler C and Hoffmann KP. Visual receptive field properties in kitten pretectal nucleus of the optic tract and dorsal terminal nucleus of the accessory optic tract. *J Neurophysiol* 70: 814–827, 1993.

Fan TX, Weber AE, Pickard GE, Faber KM, and Ariel M. Visual responses and connectivity in the turtle pretectum. *J Neurophysiol* 73: 2507–2521, 1995.

Fite KV. Pretectal and accessory-optic visual nuclei of fish, amphibia and reptiles: themes and variations. *Brain Behav Evol* 26: 71–90, 1985.

Fite KV, Brecha N, Karten HJ, and Hunt SP. Displaced ganglion cells and the accessory optic system of pigeon. *J Comp Neurol* 195: 279–288, 1981.

Fite KV, Kwei-Levy C, and Bengston L. Neurophysiological investigation of the pretectal nucleus lentiformis mesencephali in *Rana pipiens*. *Brain Behav Evol* 34: 164–170, 1989.

Follett KH and Mann MD. Effective stimulation distance for current from macroelectrodes. *Exp Neurol* 92: 75–91, 1986.

Gamlin PDR and Cohen DH. Retinal projections to the pretectum in the pigeon (*Columba livia*). *J Comp Neurol* 269: 1–17, 1988a.

Gamlin PDR and Cohen DH. Projections of the retinorecipient pretectal nuclei in the pigeon (*Columba livia*). *J Comp Neurol* 269: 18–46, 1988b.

Garey LJ and Powell TP. The projection of the retina in the cat. *J Anat* 102: 189–222, 1968.

Gibson JJ. The visual perception of object motion and subjective movement. *Psychol Rev* 61: 304–314, 1954.

Gioanni H, Rey J, Villalobos J, and Dalbera A. Single unit activity in the nucleus of the basal optic root (nBOR) during optokinetic, vestibular and visuo-vestibular stimulations in the alert pigeon (*Columba livia*). *Exp Brain Res* 57: 49–60, 1984.

Giolli RA, Blanks RH, and Torigoe Y. Pretectal and brain stem projections of the medial terminal nucleus of the accessory optic system of the rabbit and rat as studied by anterograde and retrograde neuronal tracing methods. *J Comp Neurol* 227: 228–251, 1984.

Giolli RA and Guthrie MD. The primary optic projections in the rabbit. An experimental degeneration study. *J Comp Neurol* 136: 99–126, 1969.

Gottlieb MD and McKenna OC. Light and electron microscopic study of an avian pretectal nucleus, the lentiform nucleus of the mesencephalon, magnocellular division. *J Comp Neurol* 248: 133–145, 1986.

Grasse KL and Cynader MS. Electrophysiology of medial terminal nucleus of accessory optic system in the cat. *J Neurophysiol* 48: 490–504, 1982.

Grasse KL and Cynader MS. Response properties of single units in the accessory optic system of the dark-reared cat. *Brain Res* 392: 199–210, 1986.

Grasse KL and Cynader MS. The accessory optic system of the monocularly deprived cat. *Brain Res* 428: 229–241, 1987.

Grasse KL and Cynader MS. The effect of visual cortex lesions on vertical optokinetic nystagmus in the cat. *Brain Res* 455: 385–389, 1988.

Grasse KL and Cyander MS. The accessory optic system in frontal-eyed animals. In: *Vision and Visual Dysfunction. The Neuronal Basis of Visual Function*, edited by Leventhal A. New York: Macmillan, 1990, p. 111–139.

Grasse KL, Cyander MS, and Douglas RM. Alterations in response properties in the lateral and dorsal terminal nuclei of the cat accessory optic system following visual cortex lesions. *Exp Brain Res* 55: 69–80, 1984.

Hamassaki DE, Gasparotto OC, Nogueira MI, and Britto LRG. Telencephalic and pretectal modulation of the directional selectivity of accessory optic neurons in the pigeon. *Braz J Med Biol Res* 21: 649–652, 1988.

Hayhow WR, Webb C, and Jervie A. The accessory optic fiber system in the rat. *J Comp Neurol* 115: 187–215, 1960.

Hodos W, Macko KA, and Bessette BB. Near-field acuity changes after visual system lesions in pigeons. II. Telencephalon. *Behav Brain Res.* 13: 15–30, 1984.

Hoffmann KP and Distler C. Quantitative analysis of visual receptive fields of neurons in nucleus of the optic tract and dorsal terminal nucleus of the accessory optic tract in macaque monkey. *J Neurophysiol* 62: 416–428, 1989.

Hoffmann KP, Distler C, and Erickson RG. Functional projections from striate cortex and superior temporal sulcus to the nucleus of the optic tract (NOT) and dorsal terminal nucleus of the accessory optic tract (DTN) of macaque monkeys. *J Comp Neurol* 313: 707–724, 1991.

Hoffmann KP, Distler C, Erickson RG, and Mader W. Physiological and anatomical identification of the nucleus of the optic tract and dorsal terminal nucleus of the accessory optic tract in monkeys. *Exp Brain Res* 69: 635–644, 1988.

Hoffmann KP and Schoppmann A. Retinal input to direction selective cells in the nucleus tractus opticus of the cat. *Brain Res* 99: 359–366, 1975.

Hoffmann KP and Schoppmann A. A quantitative analysis of the direction-specific response of neurons in the cat's nucleus of the optic tract. *Exp Brain Res* 42: 146–157, 1981.

Hollander H, Tietze J, and Distel H. An autoradiographic study of the subcortical projections of the rabbit striate cortex in the adult and during postnatal development. *J Comp Neurol* 184: 783–794, 1979.

Holstege G and Collewijn H. The efferent connections of the nucleus of the optic tract and the superior colliculus in the rabbit. *J Comp Neurol* 209: 139–175, 1982.

Huerta MF, Weber JT, Rothstein LR, and Harting JK. Subcortical connections of area 17 in the tree shrew: an autoradiographic analysis. *Brain Res* 340: 163–170, 1985.

Ibbotson MR, Mark RF, and Maddess TL. Spatiotemporal response properties of direction-selective neurons in the nucleus of the optic tract and the dorsal terminal nucleus of the wallaby, *Macropus eugenii*. *J Neurophysiol* 72: 2927–2943, 1994.

Ibbotson MR and Price NS. Spatiotemporal tuning of directional neurons in mammalian and avian pretectum: a comparison of physiological properties. *J Neurophysiol* 86: 2621–2624, 2001.

Ilg UJ and Hoffmann KP. Functional grouping of the cortico-pretectal projection. *J Neurophysiol* 70: 867–869, 1993.

Ilg UJ and Hoffmann KP. Responses of neurons of the nucleus of the optic tract and the dorsal terminal nucleus of the accessory optic tract in the awake monkey. *Eur J Neurosci* 8: 92–105, 1996.

Itoh K. Efferent projections of the pretectum in the cat. *Exp Brain Res* 30: 89–105, 1977.

Karten HJ, Fite KV, and Brecha N. Specific projection of displaced retinal ganglion cells upon the accessory optic system in the pigeon (*Columba livia*). *Proc Natl Acad Sci USA* 74: 1752–1756, 1977.

Karten HJ and Hodos W. *A Stereotaxic Atlas of the Brain of the Pigeon* (*Columba livia*). Baltimore, MD: Johns Hopkins Press, 1967.

Karten HJ, Hodos W, Nauta WJ, and Revzin AM. Neural connections of the "visual Wulst" of the avian telencephalon. Experimental studies in the piegon (*Columba livia*) and owl (*Speotyto cunicularia*). *J Comp Neurol* 150: 253–278, 1973.

Karten HJ and Shimizu T. The origins of the neocortex: connections and lamination as distinct events in evolution. *J Cogn Neurosci* 1: 291–301, 1989.

Katte O and Hoffmann KP. Direction specific neurons in the pretectum of the frog (*Rana esculenta*). *J Comp Physiol* 140: 53–57, 1980.

Lent R. The organization of subcortical projections of the hamster's visual cortex. *J Comp Neurol* 206: 227–242, 1982.

Liu GB and Pettigrew JD. Orientation mosaic in barn owl's visual Wulst revealed by optical imaging: comparison with cat and monkey striate and extra-striate areas. *Brain Res* 961: 153–158, 2003.

Lui F, Giolli RA, Blanks RH, and Tom EM. Pattern of striate cortical projections to the pretectal complex in the guinea pig. *J Comp Neurol* 344: 598–609, 1994.

Martin JH. Autoradiographic estimation of the extent of reversible inactivation produced by microinjection of lidocaine and muscimol in the rat. *Neurosci Lett* 127: 160–164, 1991.

McKenna OC and Wallman J. Accessory optic system and pretectum of birds: comparisons with those of other vertebrates. *Brain Behav Evol* 26: 91–116, 1985a.

McKenna OC and Wallman J. Functional postnatal changes in avian brain regions responsive to retinal slip: a 2-deoxy-D-glucose study. *J Neurosci* 5: 330–342, 1985b.

Medina L and Reiner A. Do birds possess homologues of mammalian primary visual, somatosensory and motor cortices? *Trends Neurosci* 23: 1–12, 2000.

Miceli D, Gioanni H, Reperant J, and Peyrichoux J. The avian visual Wulst. I. An anatomical study of afferent and efferent pathways. II. An electrophysiological study of the functional properties of single neurons. In: *Neural Mechanisms of Behavior of the Pigeon*, edited by Granda AM and Maxwell JH. New York: Plenum Press, 1979, p. 223–354.

Morgan B and Frost BJ. Visual response properties of neurons in the nucleus of the basal optic root of pigeons. *Exp Brain Res* 42: 184–188, 1981.

Mustari MJ and Fuchs AF. Discharge patterns of neurons in the pretectal nucleus of the optic tract (NOT) in the behaving primate. *J Neurophysiol* 64: 77–90, 1990.

Mustari MJ, Fuchs AF, Kaneko CR, and Robinson FR. Anatomical connections of the primate pretectal nucleus of the optic tract. *J Comp Neurol* 349: 111–128, 1994.

Nakayama K. Differential motion hyperacuity under conditions of common image motion. *Vision Res* 21: 1475–1482, 1981.

Nieder A and Wagner H. Perception and neuronal coding of subjective contours in the owl. *Nat Neurosci* 2: 660–663, 1999.

Nogueira MI and Britto LRG. Extraretinal modulation of accessory optic units in the pigeon. *Braz J Med Biol Res* 24: 623–631, 1991.

Pereira A, Volchan E, Vargas CD, Penetra L, and Rocha-Miranda CE. Cortical and subcortical influences on the nucleus of the optic tract of the opossum. *Neuroscience* 95: 953–963, 2000.

Perrone JA and Thiele A. Speed skills: measuring the visual speed analyzing properties of primate MT neurons. *Nat Neurosci* 4: 526–531, 2001.

Pettigrew JD. Binocular visual processing in the owl's telencephalon. *Proc R Soc Lond B Biol Sci* 204: 435–454, 1979.

Pettigrew JD and Konishi M. Neurons selective for orientation and binocular disparity in the visual Wulst of the barn owl (*Tyto alba*). *Science* 193: 675–678, 1976.

Porciatti V, Fontanesi G, Raffaelli A, and Bagnoli P. Binocularity in the little owl, *Athene noctua*. II. Properties of visually evoked potentials from the Wulst in response to monocular and binocular stimulation with sine wave gratings. *Brain Behav Evol* 35: 40–48, 1990.

Pritz MB, Mead WR, and Northcutt RG. The effects of Wulst ablations on color, brightness and pattern discrimination in pigeons (*Columba livia*). *J Comp Neurol* 140: 81–100, 1970.

Reiner A, Brecha N, and Karten HJ. A specific projection of retinal displaced ganglion cells to the nucleus of the basal optic root in the chicken. *Neuroscience* 4: 1679–1688, 1979.

Revzin AM. A specific visual projection area in the hyperstriatum of the pigeon (*Columba livia*). *Brain Res* 15: 246–249, 1969.

Riley NM, Hodos W, and Pasternak T. Effects of serial lesions of telencephalic components of the visual system in pigeons. *Vis Neurosci* 1: 387–394, 1988.

Rio JP, Villalobos J, Miceli D, and Reperant J. Efferent projections of the visual Wulst upon the nucleus of the basal optic root in the pigeon. *Brain Res* 271: 145–151, 1983.

Rosenberg AF and Ariel M. Visual-response properties of neurons in turtle basal optic nucleus in vitro. *J Neurophysiol* 63: 1033–1045, 1990.

Sandkuhler J, Maisch B, and Zimmermann M. The use of local anaesthetic microinjections to identify central pathways: a quantitative evaluation of the time course and extent of the neuronal block. *Exp Brain Res* 68: 168–178, 1987.

Scalia F and Arango V. Topographic organization of the projections of the retina to the pretectal region in the rat. *J Comp Neurol* 186: 271–292, 1979.

Schoppmann A. Projections from areas 17 and 18 of the visual cortex to the nucleus of the optic tract. *Brain Res* 223: 1–17, 1981.

Shintani T, Hoshino K, Meguro R, Kaiya T, and Norita M. A light and electron microscopic analysis of the convergent retinal and visual cortical projections to the nucleus of the optic tract (NOT) in the pigmented rat. *Neurobiology* 7: 445–460, 1999.

Simpson JI. The accessory optic system. *Rev Neurosci* 7: 13–41, 1984.

Simpson JI, Leonard CS, and Soodak RE. The accessory optic system. II. Spatial organization of direction selectivity. *J Neurophysiol* 60: 2055–2072, 1988.

Simpson JI, Soodak RE, and Hess R. The accessory optic system and its relation to the vestibulocerebellum. *Prog Brain Res* 50: 715–724, 1979.

Soodak RE and Simpson JI. The accessory optic system of rabbit. I. Basic visual response properties. *J Neurophysiol* 60: 2037–2055, 1988.

Terasawa K, Otani K, and Yamada J. Descending pathways of the nucleus of the optic tract in the rat. *Brain Res* 173: 405–417, 1979.

van der Togt C and Schmidt M. Inhibition of neuronal activity in the nucleus of the optic tract due to electrical stimulation of the medial terminal nucleus in the rat. *Eur J Neurosci* 6: 558–564, 1994.

Volchan E, Rocha-Miranda CE, Picanco-Diniz CW, Zinsmeisser B, Bernardes RF, and Franca JG. Visual response properties of pretectal units in the nucleus of the optic tract of the opossum. *Exp Brain Res* 78: 380–386, 1989.

Weber JT. Pretectal complex and accessory optic system in alert monkeys. *Brain Behav Evol* 26: 117–140, 1985.

Weber JT and Harting JK. The efferent projections of the pretectal complex: an autoradiographic and horseradish peroxidase analysis. *Brain Res* 194: 1–28, 1980.

Westheimer G and McKee SP. Failure of Donders' law during smooth pursuit eye movements. *Vision Res* 13: 2145–2253, 1973.

Wild JM. The avian somatosensory system: connections of regions of body representation in the forebrain of the pigeon. *Brain Res* 412: 205–223, 1987.

Wilson P. The organization of the visual hyperstriatum in the domestic chick. II. Receptive field properties of single units. *Brain Res* 188: 333–345, 1980.

Winterson BJ and Brauth SE. Direction-selective single units in the nucleus lentiformis mesencephali of the pigeon (*Columba livia*). *Exp Brain Res* 60: 215–226, 1985.

Wylie DR and Crowder NA. Spatiotemporal properties of fast and slow neurons in the pretectal nucleus lentiformis mesencephali in pigeons. *J Neurophysiol* 84: 2529–2540, 2000.

Wylie DR and Frost BJ. Visual response properties of neurons in the nucleus of the basal optic root of the pigeon: a quantitative analysis. *Exp Brain Res* 82: 327–336, 1990.

Wylie DR, Linkenhoker B, and Lau KL. Projections of the nucleus of the basal optic root in pigeons (*Columba livia*) revealed with biotinylated dextran amine. *J Comp Neurol* 384: 517–536, 1997.

Wylie DRW and Frost BJ. The pigeon optokinetic system: visual input in extraocular muscle coordinates. *Vis Neurosci* 13: 945–953, 1996.

Yakushin SB, Gizzi M, Reisine H, Raphan T, Buttner-Ennever J, and Cohen B. Functions of the nucleus of the optic tract (NOT). II. Control of ocular pursuit. *Exp Brain Res* 131: 433–447, 2000.

Zhang T, Fu Y-X, and Wang SR. Receptive field characteristics of neurons in the nucleus of the basal optic root in pigeons. *Neuroscience* 91: 33–40, 1999.